2002-12

Narrowband filtering effects on frequency-hopped signals

Waters, Kevin A.

Monterey, Calif. Naval Postgraduate School

NAVAL POSTGRADUATE SCHOOL
Monterey, California

THESIS

NARROWBAND FILTERING EFFECTS ON FREQUENCY-HOPPED SIGNALS

by

Kevin A. Waters

December 2002

Thesis Advisor:	R. Clark Robertson
Thesis Co-Advisor:	Kyle E. Kowalske
Second Reader:	Tri T. Ha

THIS PAGE INTENTIONALLY LEFT BLANK

REPORT DOCUMENTATION PAGE			Form Approved OMB No. 0704-0188
Public reporting burden for this collection of information is estimated to average 1 hour per response, including the time for reviewing instruction, searching existing data sources, gathering and maintaining the data needed, and completing and reviewing the collection of information. Send comments regarding this burden estimate or any other aspect of this collection of information, including suggestions for reducing this burden, to Washington headquarters Services, Directorate for Information Operations and Reports, 1215 Jefferson Davis Highway, Suite 1204, Arlington, VA 22202-4302, and to the Office of Management and Budget, Paperwork Reduction Project (0704-0188) Washington DC 20503.			
1. AGENCY USE ONLY ***(Leave blank)***	**2. REPORT DATE** December 2002	**3. REPORT TYPE AND DATES COVERED** Master's Thesis	
4. TITLE AND SUBTITLE: Narrowband Filtering Effects on Frequency-Hopped Signals			**5. FUNDING NUMBERS**
6. AUTHOR(S) Kevin Waters			
7. PERFORMING ORGANIZATION NAME(S) AND ADDRESS(ES) Naval Postgraduate School Monterey, CA 93943-5000			**8. PERFORMING ORGANIZATION REPORT NUMBER**
9. SPONSORING /MONITORING AGENCY NAME(S) AND ADDRESS(ES)			**10. SPONSORING/MONITORING AGENCY REPORT NUMBER**
11. SUPPLEMENTARY NOTES The views expressed in this thesis are those of the author and do not reflect the official policy or position of the Department of Defense or the U.S. Government.			
12a. DISTRIBUTION / AVAILABILITY STATEMENT Approved for public release; distribution is unlimited			**12b. DISTRIBUTION CODE**

13. ABSTRACT ***(maximum 200 words)***

A low complexity solution to remove follower, narrowband tone jamming signals which are randomly dispersed within the bandwidth of a hop without causing non-linear phase distortions in a frequency-hopping (FH) system is explored. Forward and reverse processed narrow stopband, elliptical infinite impulse response (IIR) filters are designed and applied to known audio and digital data. Analysis focuses on narrowband filtering one hop of a FH signal in the absence of noise. The results are compared with the output of equivalent finite impulse response (FIR) filters and equivalent forward processed IIR filters. This analysis demonstrates the effectiveness of forward and reverse narrow bandstop IIR filtering to eliminate unwanted tone jamming signals while preserving the phase of the received FH signal. These results also suggest that a FH system with narrow bandstop filtering can operate reliably in the presence of a high power tone jamming signal.

14. SUBJECT TERMS Frequency-hopping, Narrowband Tone Jamming, FIR, IIR, Non-linear Phase Distortion			**15. NUMBER OF PAGES** 53
			16. PRICE CODE
17. SECURITY CLASSIFICATION OF REPORT Unclassified	**18. SECURITY CLASSIFICATION OF THIS PAGE** Unclassified	**19. SECURITY CLASSIFICATION OF ABSTRACT** Unclassified	**20. LIMITATION OF ABSTRACT** UL

NSN 7540-01-280-5500 Standard Form 298 (Rev. 2-89)
Prescribed by ANSI Std. 239-18

THIS PAGE INTENTIONALLY LEFT BLANK

Approved for public release; distribution is unlimited

NARROWBAND FILTERING EFFECTS ON FREQUENCY-HOPPED SIGNALS

Kevin A. Waters
Civilian, Department of Defense
BSEE, Clemson University, 1996

Submitted in partial fulfillment of the
requirements for the degree of

MASTER OF SCIENCE IN ELECTRICAL ENGINEERING

from the

NAVAL POSTGRADUATE SCHOOL
December 2002

Author: Kevin Waters

Approved by: R. Clark Robertson, Thesis Advisor

Kyle E. Kowalske, Co-Advisor

Tri T. Ha, Second Reader

John P. Powers
Chairman, Department of Electrical and Computer Engineering

THIS PAGE INTENTIONALLY LEFT BLANK

ABSTRACT

This thesis explored a low complexity solution to remove follower, narrowband tone jamming signals which are randomly dispersed within the bandwidth of a hop without causing non-linear phase distortions in a frequency-hopping (FH) system. Forward and reverse processed narrow stopband, elliptical infinite impulse response (IIR) filters were designed and applied to known audio and digital data. Analysis focused on narrowband filtering one hop of a FH signal in the absence of noise. The results were compared with the output of equivalent finite impulse response (FIR) filters and equivalent forward processed IIR filters. This analysis demonstrates the effectiveness of forward and reverse narrow bandstop IIR filtering to eliminate unwanted tone jamming signals while preserving the phase of the received FH signal. These results also suggest that a FH system with narrow bandstop filtering can operate reliably in the presence of a high power tone jamming signal.

THIS PAGE INTENTIONALLY LEFT BLANK

TABLE OF CONTENTS

THIS PAGE INTENTIONALLY LEFT BLANK

LIST OF FIGURES

THIS PAGE INTENTIONALLY LEFT BLANK

LIST OF TABLES

THIS PAGE INTENTIONALLY LEFT BLANK

ACKNOWLEDGMENTS

I would like to thank William Hatch for his time and editorial comments related to this paper. He definitely inspired me to become a better writer after his first bit of advice was for me to sign up for a writing course once this thesis was submitted. I would also like to thank Professor R. C. Robertson for enduring the burden of thesis advisor. His comments and direction definitely added to the quality of this paper. Finally, after three local advisors, two thesis topics, and many dead-end paths, I would like to thank Kyle Kowalske for not ignoring me in line at the Baltimore Washington International airport. I never knew that having lunch in Phoenix would change the direction of my life for six months. I am also grateful that he remained a faithful government employee and did not seek employment in the private sector, like previous advisors.

THIS PAGE INTENTIONALLY LEFT BLANK

EXECUTIVE SUMMARY

This thesis investigates the effects of removing follower, narrowband tone jamming signals from the hop-band of a frequency-hopping signal using a low complexity solution which minimizes phase distortion and processing time.

Forward and reverse processed narrow bandstop infinite impulse response (IIR) filters were designed to remove tone jamming signals while preserving the phase of the received signal. The results were compared to equivalent finite impulse response (FIR) filters and forward processed IIR filters.

The results of this research show how narrow, bandstop IIR filtering a tone interferer could degrade the received signal if the filter disturbs the phase of the signal. Leaving the tone in the spectrum for processing could yield better results if the narrow bandstop filter has a nonlinear phase response.

In addition, implementing narrow bandstop FIR filters requires a significant number of taps and processing capability. Equivalent forward processed IIR filters require fewer taps to implement but cause unacceptable phase distortion. Equivalent forward and reverse processed IIR filters preserve the phase of the signal, require less processing capability than a FIR filter, and remain low in complexity to implement. Typical processing times for the IIR filters were measured in minutes, while the FIR filters were measured in hours.

Finally, comparing the bit error ratio (BER) for varying data rate frequency shift-keyed (FSK) signals, we found that narrow bandstop filtering near the FSK tone causes increases in the BER. The BER increases dramatically for higher data rates.

The work described in this thesis provides guidelines for the development of robust, low complexity processors capable of removing the effects of narrowband tone

jammers. The results also can be used to predict the performance of current frequency-hopping systems in the presence of narrowband tone jammers.

I. INTRODUCTION

What do perforated paper rolls, player pianos, and a Vienna born actress have in common? They all contributed to the invention and implementation of frequency-hopping technology [1]. In frequency-hopped (FH) spread spectrum, rather than transmit all information (data or voice) with the same carrier frequency, the carrier frequency is changed (hopped) periodically according to some pre-designated (but apparently random to a third party observer) code (a pseudo-random sequence).

Hedy Lemarr, actress and inventor, and George Antheil, avant-garde composer, proposed the idea of frequency-hopping in 1942. The concept of frequency-hopping was easy to envision, but synchronization of the transmitter and receiver posed a problem [2]. Antheil's work history included a synchronization method he developed to play 16 player pianos for the musical score in the film "Ballet mécanique." The key to synchronizing the pianos was the use of perforated paper rolls [1].

Lemarr and Antheil obtained a patent for their idea, but it was not until 1962, three years after the original patent expired, that the U.S implemented the idea for military communication systems onboard ships [2].

The use of frequency-hopping systems has increased dramatically since its inception in 1962. The Single Channel Ground-Airborne Radio System (SINCGARS) and Panther are examples of frequency-hopping tactical radios in current production. Information obtained from open literature states that the SINCGARS operates in the 30-88 MHz frequency range, while the Panther operates from 30-108 MHz. The SINCGARS is capable of frequency-modulated (FM) voice and point-to-point data or packet-switched data transmissions with data rates up to 16 kbps while hopping over 2 to 2,320 different frequencies [3].

The advantage of a frequency-hopping signal is that it is relatively jam and intercept resistant. This feature is used widely in military communications where the risk of either enemy jamming or intercept is great. It is also used in the mobile

communication industry as a multiple access technique where systems are required to handle high capacity data reliably in an urban setting [1].

Frequency-hopping (FH) communication systems have become an important component of military communications strategy. FH systems offer an improvement in performance when the communication system is attacked by hostile interference. FH systems also reduce the ability of a hostile observer to receive and demodulate the communications signal [4]. FH systems are susceptible to a number of jamming threats, such as noise jammers and narrowband, single or multitone jammers. This thesis reports on the use of band rejection filters to counter single or multitone jammers.

If all frequency hops are to be jammed, the jammer has to divide its power over the entire hop band, thus lowering the amount of received jamming power at each hop frequency. Unfortunately, if the tone jamming signal has a significant power advantage, reliable communications will not be possible [5]. Even when the jamming tones experience fading, reliable communications are not possible when the jamming signal has a significant power advantage [4]. If the FH signal has a sufficient hop range, received jamming power will be negligible. If a tone jammer is focused on a particular portion of the FH bandwidth, its power may adversely impact communications. A possible anti-jamming strategy is use a narrow bandstop filter to remove the tone from the received signal spectrum.

In [6], a method for filtering tone jammers from a frequency-hopping spread spectrum signal based on the undecimated wavelet transform is presented. This technique isolates the jamming signal using frequency shifts to confine it to one transform subband. This method to remove a jamming signal is significantly more complicated than using a narrow bandstop filter.

In [7], a rejection scheme based on least-mean square estimation techniques using a tapped delay line to implement either a one-sided prediction-error filter or a two-sided filter is presented. Another technique described is transform domain processing. This scheme uses a tapped delay line and a surface acoustic wave device with a chirp impulse response built into the taps to implement a real-time Fourier transformer. The two

techniques presented are more complicated to implement than the method proposed in this paper.

To the best of the author's knowledge, this is the first time a zero-phase IIR filter has been used for interference reduction in FH systems. Previous research has investigated higher complexity techniques to remove narrowband, jamming signals. In [8], attempts to phase-lock to the jamming signal and subtract it were discussed. This technique was analyzed without additive white Gaussian noise. A similar technique [9] using additional circuitry to better estimate the jamming tone before subtraction was also analyzed without additive white Gaussian noise. The phase-locked loop is much more susceptible to additive white Gaussian noise than the zero-phase IIR filter proposed in this paper. The zero-phase IIR filter is also a much lower complexity technique to implement.

There are two ways to design a narrow bandstop filter. These are finite impulse response (FIR) and infinite impulse response (IIR) filters. FIR filters are stable with a linear phase response and a constant group delay. IIR filters may be unstable and have a nonlinear phase response with a frequency dependent group delay. Narrow bandstop FIR filters require a significantly larger number of taps to implement than an equivalent IIR filter.

In order to remove the jamming signal, we will investigate the following three approaches:

- FIR filters,
- IIR filters with only forward processing, and
- IIR filters with forward and reverse processing.

A narrowband FIR filter preserves the phase of the signal but experiences a significant group delay because of the large number of taps required. An equivalent IIR filter has fewer taps and thus would consume less computer resources. The drawback in this approach is the signal distortion caused by the nonlinear phase response of the IIR filter. This problem is avoidable if the third approach is used. An IIR filter using forward and

reverse processing removes the signal distortion. The result is a process that preserves the phase content of the signal and is computationally less intensive than the FIR approach.

The FIR approach provides delayed real-time processing capability. The forward and reverse processed IIR filter processes overlapping batches of data in near real-time. In the specific narrowband case presented in this paper, the batch delay was much smaller than the FIR delay.

In this thesis, a low complexity solution to remove follower, tone jamming signals without causing non-linear phase distortions in the received signal is investigated. Actual jamming tones will not be applied in the analysis. The approach is to implement forward and reverse processed elliptical IIR filters that remove phase distortions caused by the non-linear phase response of the IIR filters. These results are compared with the output of equivalent FIR filters and equivalent forward processed IIR filters. These comparisons show that forward and reverse processing elliptical IIR filters do not significantly degrade the quality of the received signal.

II. NARROW BANDSTOP FILTER EFFECTS

In this chapter we explore the effects of using FIR and IIR bandstop filters to eliminate narrowband interferers. A brief discussion of the generation of the frequency modulated (FM) audio and frequency-shift keyed (FSK) test signals is given. An overview of digital filters and their advantages is also discussed. Finally, the results of applying the FIR and IIR filters to the test signals are presented.

A. METHODOLOGY

The effects of FIR and IIR notch filters applied to both analog and digital modulations are discussed in this section. By using a known audio signal and known digital data sequence, it is easy to hear and see the results of notch filtering the respective modulation types. The initial scope of this study was to look only at the effects filtering had on audio signals, but it soon became apparent that a quantitative measure of the effect would better support what was being heard from the filtered audio file. This decision led to the use of an FSK signal, in addition to the audio, so that bit error ratio (BER) calculations could be made. All simulations mentioned are based on scripts written and executed in Matlab.

The analog (FM) simulation is based on the block diagram shown in Figure 1. The audio source is FM modulated, filtered, demodulated and then passed to the computer's speaker to listen for signal degradation.

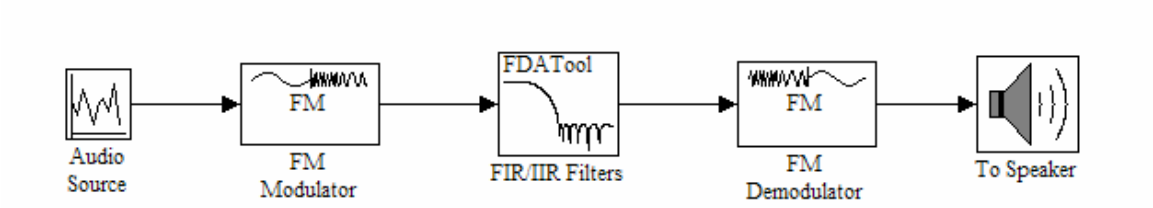

Figure 1. Block diagram of FM simulation.

The digital (FSK) simulation is based on the block diagram shown in Figure 2. The FSK simulations encompass a number of factors in that they use ten different random

seeds in the random data generator to generate the underlying data for analysis. The seeds are specified so that they are the same for each independent run. The generated data is modulated, filtered, demodulated and then passed to a BER calculator. The result is one BER matrix that, when averaged, yields a BER curve that is the result of ten independent runs of the signal at a particular data rate. This method provides a better sampling of the effects of filtering.

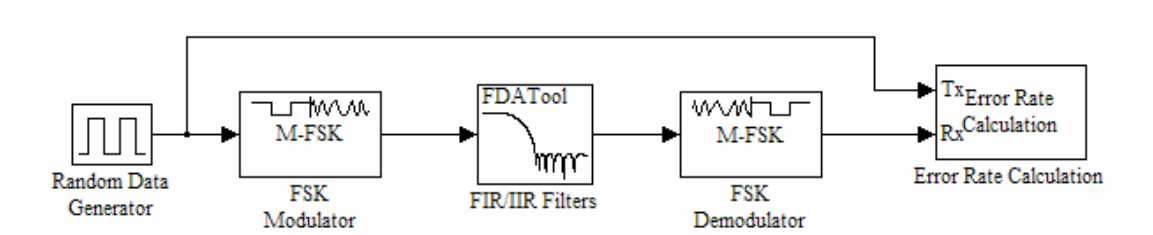

Figure 2. Block diagram of FSK simulation.

In both the FM and FSK simulations, the FIR/IIR filter block is where the modulated signal is processed using a FIR filter, an IIR filter with forward processing, or an IIR filter with forward and reverse processing.

Analysis was constrained to one hop of a FH signal. To simulate the effects of tone jamming, filters were sequentially and symmetrically applied in an alternating pattern around the center frequency of the hop. This analysis is also a worst case scenario for narrowband interference since we are assuming all interference occurs within the bandwidth of one hop.

B. TEST SIGNALS

Two test signals were chosen such that each occupies approximately 25 kHz of bandwidth. This bandwidth was chosen to closely resemble the bandwidth of one hop for a particular type of frequency-hopping radio. This constraint ensures consistent results when applying the filters to the FM and FSK signals. In each case, the modulated signal has a center frequency of 250 kHz and a sampling frequency of 1 MHz.

1. Frequency Modulated Audio Signal

The FM signal was generated using audio from a recorded song. The audio was originally sampled at 44.1 kHz so that its baseband bandwidth is approximately 22 kHz. For analysis this baseband audio was bandlimited by low-pass filtering it to first 4 kHz and then 10 kHz bandwidths. Each bandlimited version was modulated and evaluated to determine which is more adversely affected. As expected, the 4 kHz version was more susceptible to the filtering than the 10 kHz version.

2. Frequency Shift-keyed Signal

The FSK signal was generated using a random sequence of binary data generated in Matlab. The frequency deviation was set at 12.5 kHz with a data rate that varied from 1953.125 to 62500 bits per second (bps). The various data rates used are listed in Table 1.

Table 1. Data rates used to generate the FSK signals.

Index	Data rate (bits per second)
1	1,953.125
2	3,906.25
3	7,812.5
4	10,000
5	15,625
6	25,000
7	31,250
8	50,000
9	62,500

The FSK signal was generated with various data rates to see how the narrowband filters affect BER as the data rate increases. The results show that as data rate increases, the BER increases also. The results of this analysis are presented later in this chapter.

C. DIGITAL FILTERS

In this Section we discuss the use of digital filters, some advantages and disadvantages of the various filter types, and how the filters were designed and implemented for this thesis.

1. Overview

The basic digital filter structure is shown in Figure 3. The filter stages on the top half take previous input samples and feed them forward. This process allows the filter to have memory of past input values. Each past and present input value is multiplied by gain coefficients and summed to produce the filter output.

The lower half feeds back past output values, multiplies them by gain coefficients, and adds them to the current output.

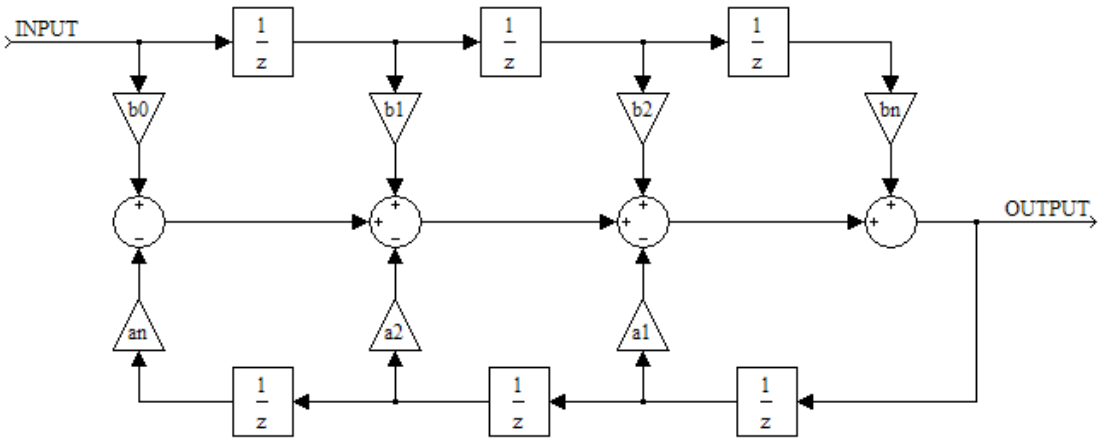

Figure 3. Block diagram of a digital filter [After Ref. 10].

FIR filters contain only the feed-forward terms. An IIR filter has feedback terms and may or may not contain feed-forward terms [10].

2. FIR versus IIR

The discussion that follows describes the advantages and disadvantages of FIR and IIR filters. The discussion is summarized at the end of this section in Table 2.

FIR filters use only feed-forward terms to process the input samples. This design is very stable because there are no gain coefficients in the feedback loop (i.e., no *a* terms which could cause oscillations.) IIR filters may be more unstable since there are non-zero values in the feedback loop which could cause oscillations in the filter output [10].

FIR filters can also be designed to have exact linear phase and group delay, whereas IIR filters have a non-linear phase response and a varying group delay [10]. Having linear phase and a constant group delay is desirable, but the tradeoff is a much larger filter and a need for greater processing capability. The use of IIR filters can cause phase distortion, leading to intersymbol interference. It can also cause dispersion in the output due to non-linearities in the group delay of the filter. Nonlinear group delay causes some frequencies to arrive at the output before other frequencies.

FIR filters are also less sensitive to rounding errors in the gain coefficients. This is true because the feedback loop for IIR filters reintroduces any errors that occur in the feed-forward section. The reintroduction of errors is compounded when applied to the gain coefficients and summed with the other values. This is not the case with FIR filters. The samples are fed through the system once, avoiding the reintroduction of errors.

FIR filters generally require more stages than an IIR to implement, especially if sharp cutoff bands are required. The large number of stages requires more processing and more memory to perform the computations. IIR filters, on the other hand, have fewer stages for the same filter specifications. This smaller design size speeds up the processing and requires less memory.

The previous discussion is summarized in Table 2.

Table 2. FIR versus IIR filters

Property	FIR Filter	IIR Filters
Stability	Always stable	Requires incorporation of stability constraint
Phase Linearity	Can be exact Linear	Non-linear
Sensitivity to coefficient inaccuracy	Low sensitivity	High sensitivity
Computation	Large number of multiplications and additions	Small number of multiplications and additions
Storage	High amount of storage	Low amount of storage

3. Design and Implementation

The FIR and IIR filters used for the simulations were designed using the Filter Design and Analysis Toolbox in Matlab. To meet the requirements of this research, the filters had to be designed to have a very narrow stopband (50 Hz, 100 Hz, and 200 Hz) with sharp transitions. The IIR and FIR filters were designed by specifying the parameters shown in Figure 4. In all cases, IIR and FIR, the magnitude parameters A_{pass1}, A_{pass2}, and A_{stop} were constrained to 0.5 dB, 1.0 dB, and 40 dB, respectively. The passband parameters F_{pass1}, F_{stop1}, F_{stop2}, and F_{pass2} were varied to achieve the desired frequency response. A total of 36 FIR filters and 36 IIR filters were designed to use in the simulations. Each group of 36 filters is broken into three sets of twelve filters. Each set of twelve filters has center frequencies of 238, 240, 244, 247, 249, 250, 252, 254, 256, 258, 260, and 262 kHz with null bandwidths of 50, 100, or 200 Hz. Since there were a large number of filters designed, only one FIR filter and one IIR filter will be presented in the text.

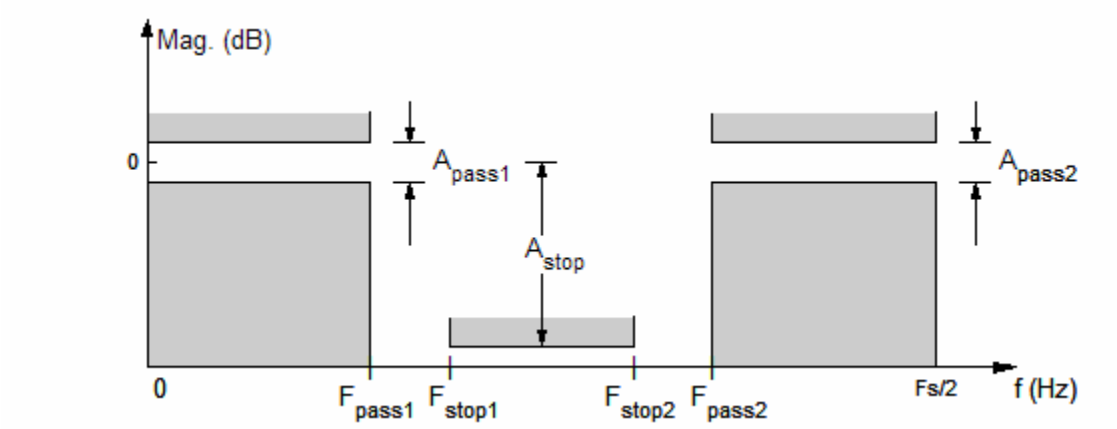

Figure 4. Filter model showing specifiable parameters.

The FIR filters were designed to achieve a minimum filter order using a Kaiser window. Other filter models were limited in the amount of flexibility the designer had on parameter specification. The passband parameters F_{pass1}, F_{stop1}, F_{stop2}, and F_{pass2} specified to design the filter in Figure 5 are 249.825 kHz, 249.900 kHz, 250.100 kHz, and 250.175 kHz, respectively. These parameters resulted in the design of a filter with a center frequency of 250 kHz and a null bandwidth of 200 Hz (see Figures 5 and 6). Figure 6 is a zoomed in depiction of Figure 5 to show the steepness of the notch. Notice the linear phase response in Figure 5. This FIR filter has a minimum order of 29,766 taps.

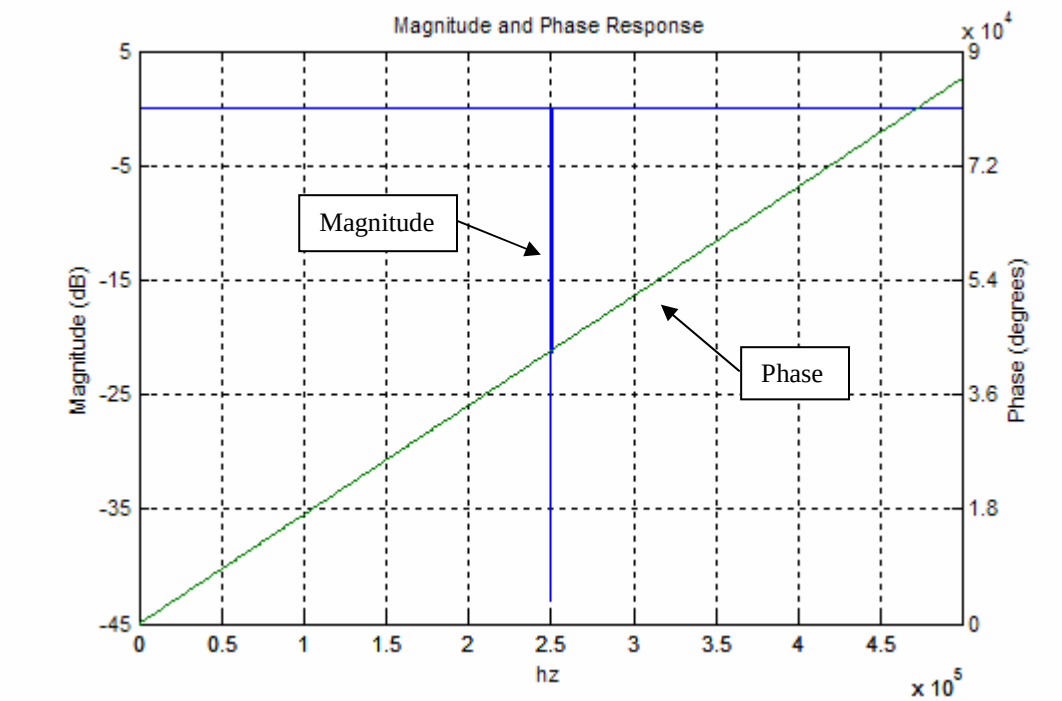

Figure 5. Plot of magnitude and phase response for a narrowband Kaiser windowed FIR notch filter with a center frequency of 250 kHz and null bandwidth of 200 Hz.

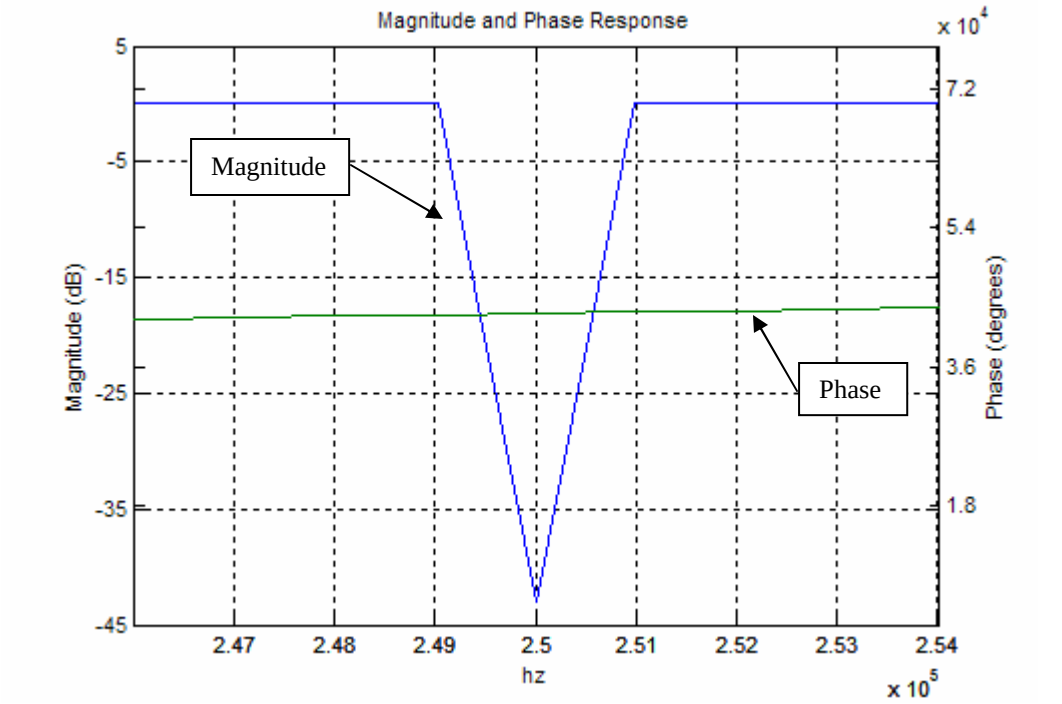

Figure 6. (Zoomed view) Plot of magnitude and phase response for a narrowband Kaiser windowed FIR notch filter with a center frequency of 250 kHz and null bandwidth of 200 Hz.

Another characteristic of FIR filters is their constant group delay (Figure 7), which is a result of its linear phase response. The group delay for the FIR filter in Figure 5 is 14,883 samples. This high value is a result of the large number of taps needed to implement the filter design.

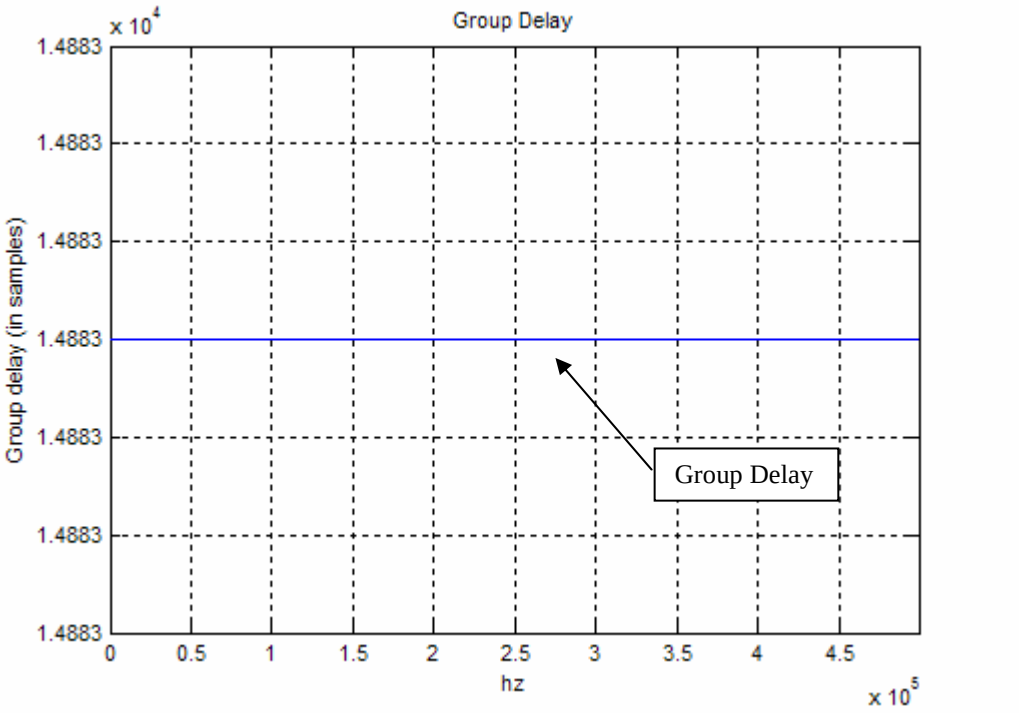

Figure 7. Group delay for a narrowband Kaiser windowed FIR notch filter with a center frequency of 250 kHz and null bandwidth of 200 Hz.

An IIR filter can be designed to have extremely sharp transitions with fewer taps than an equivalent FIR filter. Unlike FIR filters, IIR filters are not guaranteed to be stable or have linear phase response. This phase distortion causes problems with analog and digital signals. Although nulling a jamming tone in a frequency-hopped signal will theoretically improve the system performance, distortions caused by a filter with a nonlinear phase could increase BER more than a tone jammer.

An elliptic filter type was chosen because it provides increased steepness in the transition region by allowing some ripple in the passband [11]. Also, this was the only type of IIR filter that achieved the desired specifications and remained stable. The IIR filters were designed by specifying the same parameters as the FIR filters. The IIR filter presented has a center frequency of 250 kHz and a null bandwidth of 200 Hz.

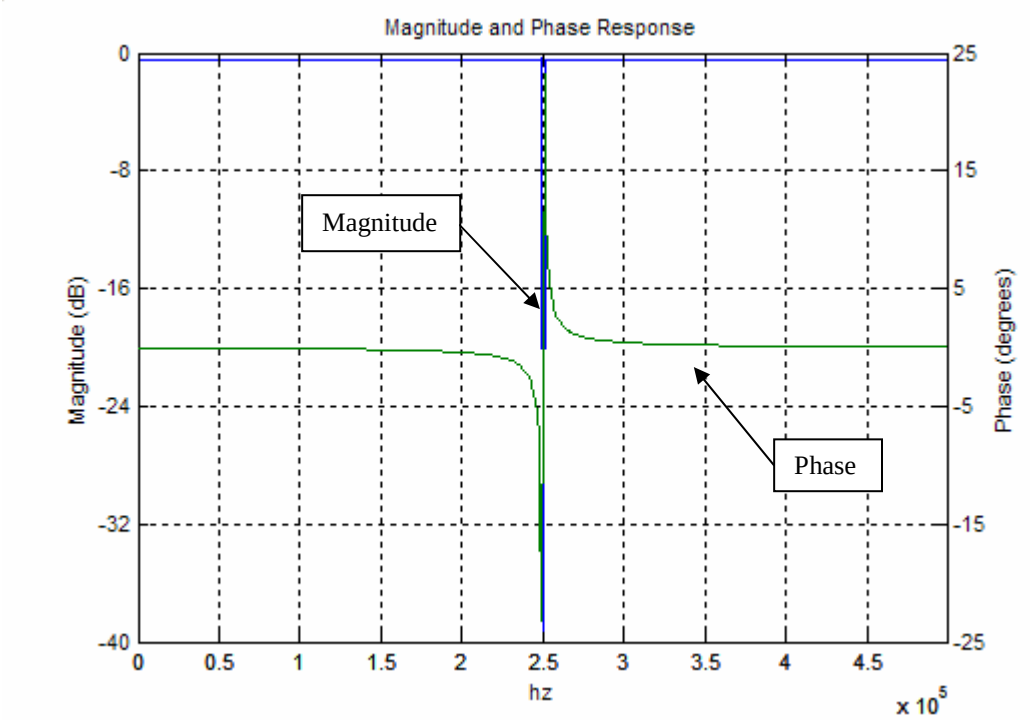

Figure 8. Plot of magnitude and phase response for a narrowband elliptic IIR notch filter with a center frequency of 250 kHz and null bandwidth of 200 Hz.

Magnitude and phase response plots for an elliptic IIR notch filter with a center frequency of 250 kHz and a null bandwidth of 200 Hz are shown in Figures 8 and 9. Figure 9 is a zoomed-in depiction of Figure 8 to show the steepness of the notch. Notice how nonlinear the phase response is compared to the phase response of the FIR filter shown in Figures 5 and 6. This IIR filter has a minimum filter order of eight taps. This filter design is much easier to implement, but the tradeoff is the nonlinear phase response. By using forward and reverse processing to remove any nonlinearities in the phase, we gain a much more robust filtering system.

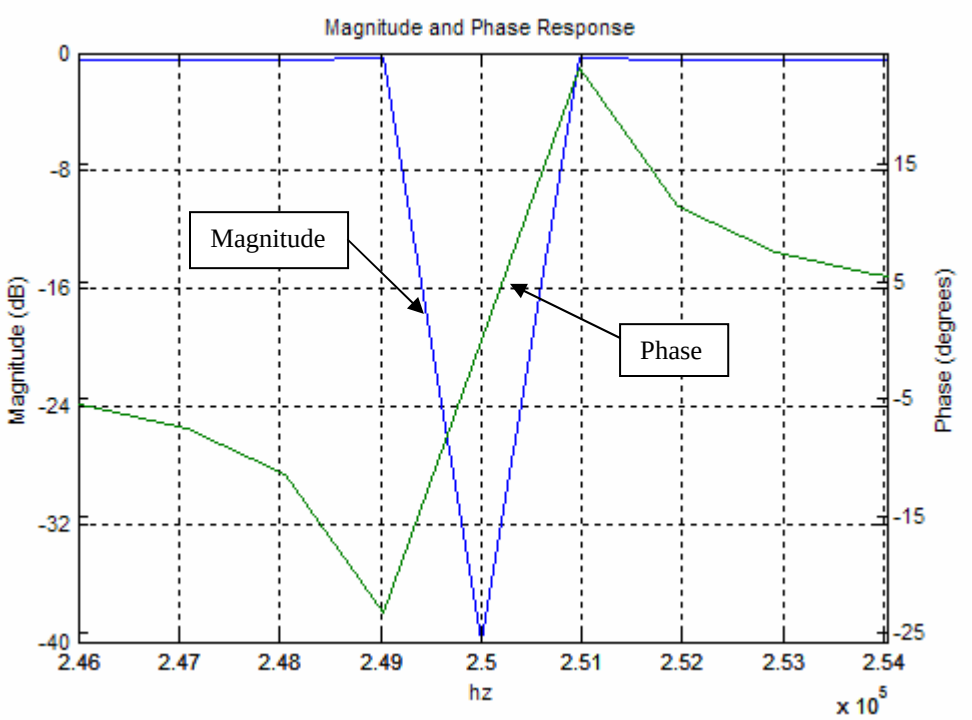

Figure 9. (Zoomed view) Plot of magnitude and phase response for a narrowband elliptic IIR notch filter with a center frequency of 250 kHz and null bandwidth of 200 Hz.

Group delay is also a major contributor to intersymbol interference and phase distortion in the signal. Recall the constant group delay associated with the FIR filter in Figure 7. This is not the case for the IIR filter in Figure 8. Its group delay, seen in Figure 10, is actually frequency dependent. This frequency dependence causes certain frequencies to arrive at the output before others, resulting in audio distortion or intersymbol interference. The effect of this is removed when forward and backward processing is used.

Comparing group delays for the narrowband FIR and IIR filters designed, the maximum group delay for the IIR filter is much smaller than the constant group delay of its equivalent FIR filter. The forward and reverse processed IIR filters have zero group delay.

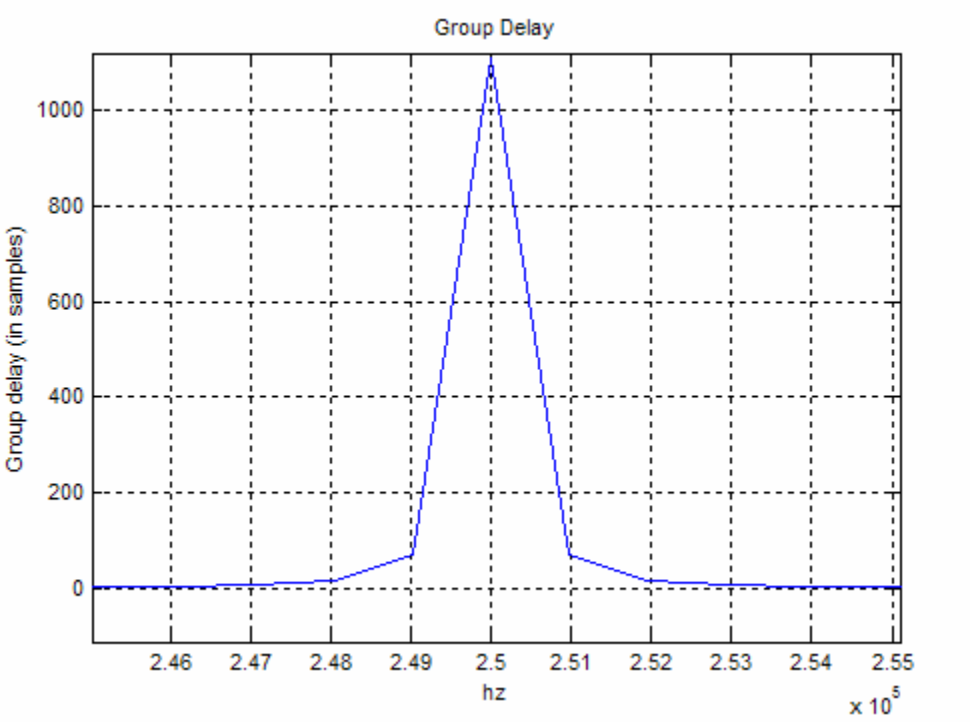

Figure 10. Group delay for a narrowband elliptic IIR notch filter with a center frequency of 250 kHz and null bandwidth of 200 Hz.

The various frequencies, bandwidths, and orders associated with the filters designed for this research are shown in Table 3. Since each set of filters for a corresponding null bandwidth was designed with the same parameters, only shifted in frequency, the associated filter orders are the same.

Table 3. Summary of FIR and IIR filter order and group delay.

Center Frequency (kHz)	Null Bandwidth (Hz)	FIR Order	FIR Group Delay	IIR Order	IIR Group Delay
238, 240, 244, 247, 249, 250, 252, 254, 256, 258, 260, 262	50	44,648	22,324	6	Variable
	100	22,324	11,162	6	Variable
	200	29,766	14883	8	Variable

D. APPLICATION OF FILTERS TO TEST SIGNALS

We will now investigate the performance of a narrow bandstop IIR filter using both the *filter* and *filtfilt* commands in Matlab. The *filter* command passes the input signal through the filter one time. In this case, the filter response can be written as $a(f) + jb(f)$ where $j = \sqrt{-1}$, and the variables $a(f)$ and $b(f)$ are dependent on the frequency of the input signal. The magnitude of the filter response is $\sqrt{a(f)^2 + b(f)^2}$ and the phase is $\tan^{-1}\left(b(f)/a(f)\right)$. For a FIR filter the phase varies linearly as a function of frequency. IIR filters have a non-linear phase response which can cause signal distortion.

The *filtfilt* command filters the input signal once in the forward direction, then inverts the output and filters the signal again in the reverse direction. In this case, the filter response can be written as $[a(f) + jb(f)] \times [(a(f) - jb(f)]$. The magnitude of the filter response is $a(f)^2 + b(f)^2$ and the phase is zero. Thus the *filtfilt* command does not have any non-linear phase distortions even when an IIR filter is used.

For the simulations that follow, the nonlinear phase response of the IIR filters with forward processing will be demonstrated using the Matlab *filter* command, while the

filtfilt command will be used to demonstrate the zero phase response of the IIR filter with forward and reverse processing.

1. Method

First, the IIR filters were applied to the FM voice and FSK modulated signals using forward processing to see how the voice and digital data are affected by the nonlinear phase response. The same simulations were run using forward and reverse processing to show how the nonlinear phase response can be removed to improve the voice and digital data. In each simulation, twelve IIR filters with specific null bandwidths (50, 100, or 200 Hz) were applied to the FM voice and FSK signals in a serially symmetric order. The first filter was applied at a center frequency of 250 kHz. The second filter was applied at a center frequency of 249 kHz. The remaining filters were applied symmetrically around the center frequency of the FSK signal (i.e., 250, 249, 252, 247, 254, 244, 256, 240, 258, 238, 260, and 262 kHz, respectively.) The result of applying twelve IIR filters to the FSK signal is shown in Figure 11. The two FSK tones noted in Figure 11 show the frequency deviation of the FSK signal.

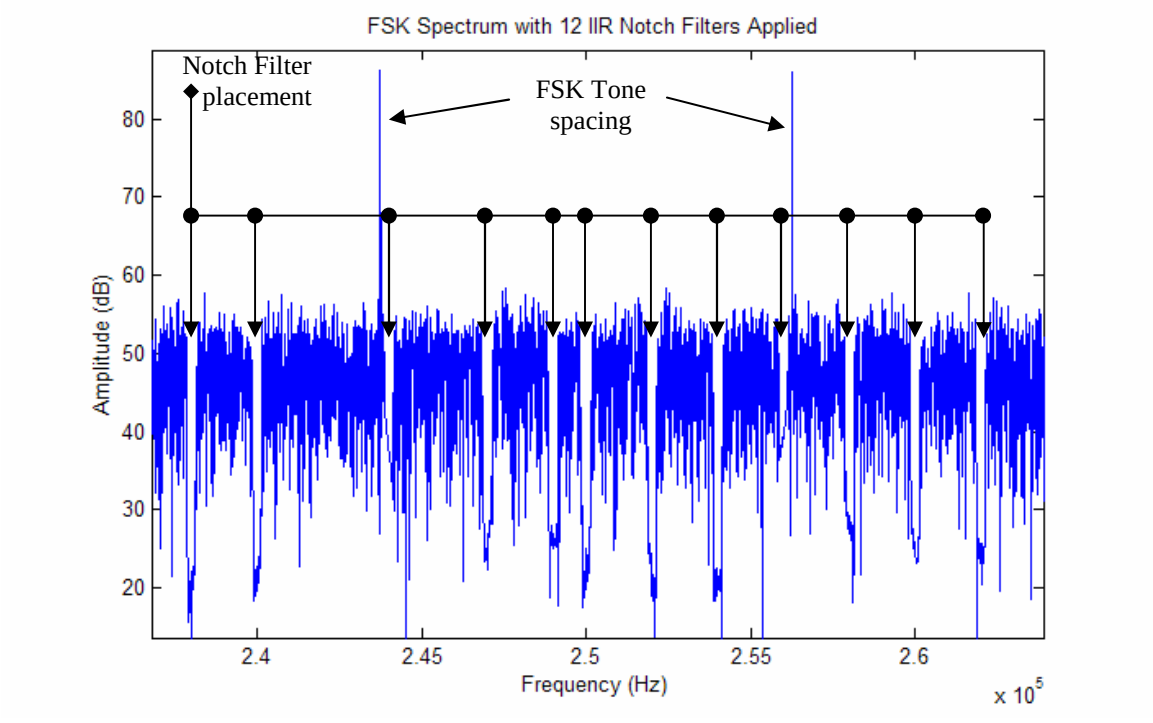

Figure 11. FSK spectrum with twelve IIR notch filters applied.

The FIR filter simulations were run once due to the computationally intensive processing involved in obtaining a solution.

2. Results

The audio processing results were evaluated qualitatively by listening to the output signal. The apparent distortion increased as more narrowband IIR filters were applied. The distortion was reduced with forward and reverse IIR processing.

Similar results were observed in the FSK simulations seen in Figure 12. When the binary data was processed through the IIR filters using forward processing (upper part of Figure 12), the BER increased quickly as more filters were applied. When the binary data was processed forward and backward through the filter, the BER improved considerably. The dotted lines in Figure 12 show the BER progression as more filters are applied for a particular data rate. The actual data points are represented by the circles. For forward processing, the lower data rates experienced less distortion and, therefore, a lower BER. The first four data rates (Table 1, index values 1-4) experienced a BER of zero until the sixth filter was applied. The last five data rates (Table 1, index values 5-9) experienced noticeable BER values after one or two filters were applied. Notice there are only a few data points represented in the lower right-hand side of Figure 12. This occurs because many of the BER data points for the forward and reverse processed IIR filter are zero at lower data rates. In fact, noticeable BER values are not apparent until the last four data rates (Table 1, index values 6-9) are simulated. Even then, BER values are zero until four or more filters are applied to the FSK signal.

In Figure 11, there is one notch filter just to the right of the low frequency tone and one notch filter just to the left of the high frequency tone. Remember that the filters are applied symmetrically starting at a center frequency of 250 kHz. When we apply the sixth filter next to the low frequency tone, the overall system BER spikes to about 10^{-1} with forward processing and to about 10^{-4} with forward and reverse processing. Once the seventh filter is applied next to the high frequency tone, the BER is reduced about one order of magnitude. This can be seen in Figure 12.

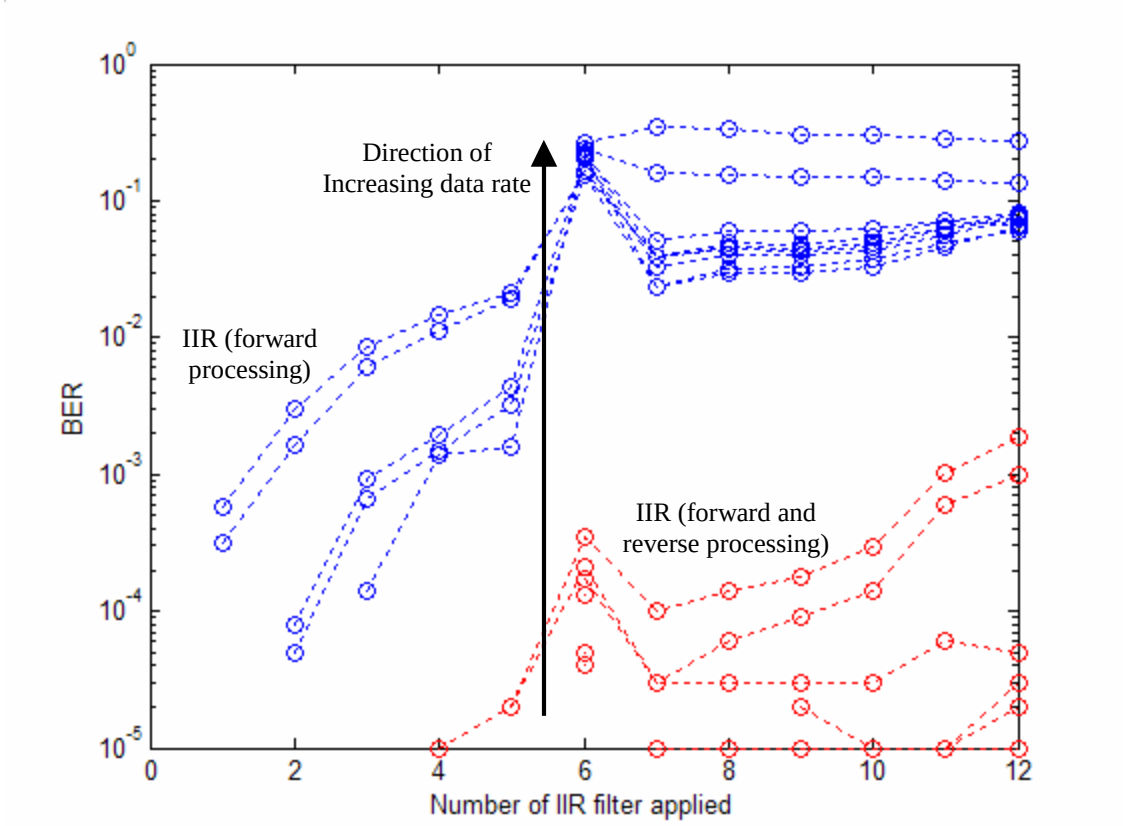

Figure 12. BER versus number of IIR filters applied for various data rates.

These results are consistent with what we should see based on the characteristics of FIR and IIR filters. Note that both the FIR filter and the forward and reverse IIR filter introduce a time delay. For the FIR filter, this delay is equal to the sample interval times half the number of taps. The time delay introduced by a forward and reverse IIR filter is equal to two times the length of the time slice being filtered. As long as the time slice is of a reasonable size, the forward and reverse processed IIR filter will take less time than the FIR filter to produce a result.

In this Chapter we discussed the advantages and disadvantages of FIR and IIR filters. We discussed the effects of phase distortion when narrowband IIR filters are applied to a signal. We also showed how these effects are eliminated using forward and reverse processing.

In the next Chapter we discuss how we generated snapshots of FH signals for follow-on research.

III. FREQUENCY-HOPPING SIMULATION

In this chapter we discuss the methods used to obtain digital snapshots of actual frequency-hopping signals in narrowband and wideband operating modes. A brief description about the folding frequency of digitizers and how they were used to obtain the snapshots is covered. We end with a brief discussion on how these snapshots can be used to help further research in this area.

A. METHODOLOGY

Detailed simulations of FH signals with known underlying data are desired to provide developers a way to test new algorithms and processing techniques. The preceding chapter focused on the effects of notch filtering one hop. These test signals will provide an opportunity to test these results by looking at a number of hops. It also provides the ability for noise to be added to the system to see the effects of notch filters in an environment with varying signal-to-noise ratios (SNR). Finally, the test signals can be used to study the effects of channel fading and multipath.

Obtaining good quality digital snapshots of actual FH signals sometimes required using the digitizer out of its normal operating range. Unless explicitly stated, the digitizer was used under normal Nyquist conditions.

B. BANDWIDTH LIMITATION OF DIGITIZERS

The amount of bandwidth a digitizer can process is limited by its sampling frequency, F_s. The *Nyquist sampling theorem* states:

> If the highest frequency contained in a continuous time signal $x(t)$ is f_{max}, then $x(t)$ can be recovered exactly from its sample values provided the sampling frequency is such that $F_s > 2\, f_{max}$ [12].

For example, if a digitizer has sampling frequency F_s only frequencies f_x less than F_s /2 will be recovered exactly. In Figure 13, f_1 and f_2 are below F_s /2 so, based on the Nyquist sampling theorem, the digitizer output will be recovered exactly.

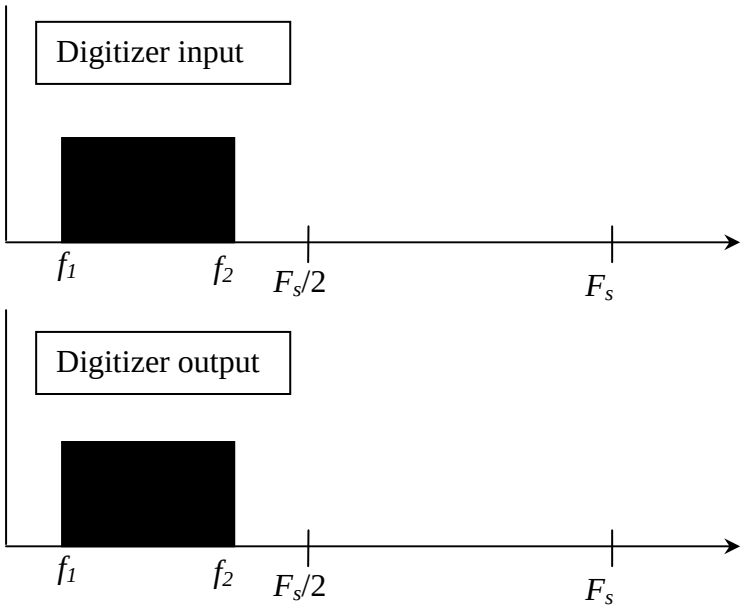

Figure 13. Digitizer input and output spectrum when sampled at Nyquist.

If f_x is greater than $F_s/2$, it is aliased or "folded" back into the digitizer spectrum at a frequency specified by $kF_s \pm f_x$, where k is an integer [12]. An example of this is seen in Figure 14. The spectrum spans f_1 to f_2. The input spectrum above $F_s/2$ is folded back into the digitizer spectrum, denoted by the hashed area. The spectrum from f_1 to $F_s - f_2$ is digitized properly, but the spectrum from $F_s - f_2$ to $F_s/2$ is distorted due to the input spectrum being folded on top of the original spectrum. This is not desirable.

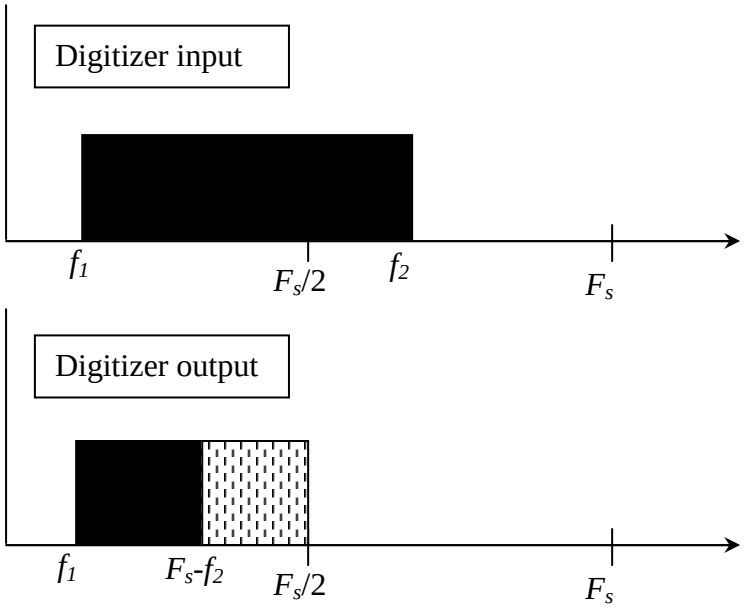

Figure 14. Digitizer input and output spectrum when input spans the Nyquist frequency.

Sometimes the desired frequency spectrum is outside of the digitizer's normal frequency range. In this case, the folding frequency can be used as an alternative to obtain the signal spectrum. This method is shown in Figure 15. The input bandwidth is above the Nyquist frequency, so the entire bandwidth is folded back into the spectrum of the digitizer. Notice that the spectrum does get inverted when using this method.

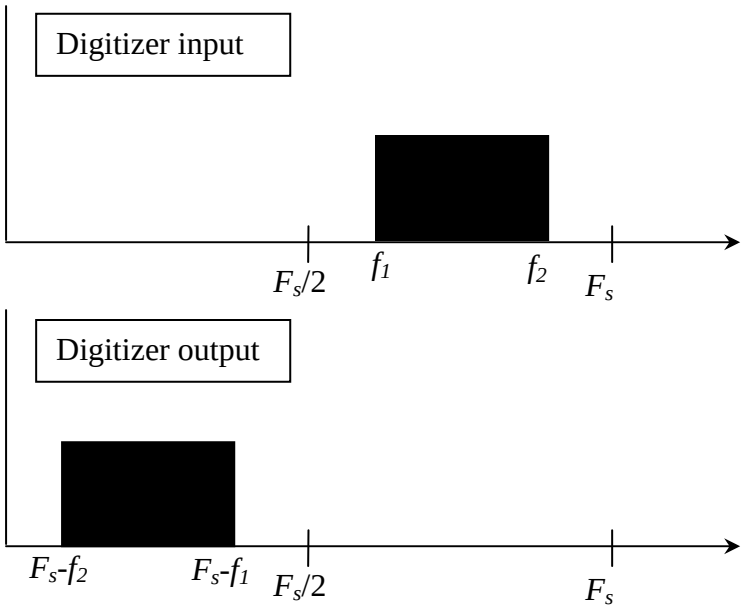

Figure 15. Digitizer input and output spectrum when the input is above the Nyquist frequency.

C. DIGITIZING THE NARROWBAND MODE

There were four equipment configurations used to digitize the narrowband FH signal. The FH radio transmits within a 6.4 MHz bandwidth in narrowband mode. The digitizer used to take snapshots of the narrowband FH signal has a maximum sampling frequency, F_s, of 64 MHz but is capable of lower sampling frequencies such as 20 MHz and 40 MHz. The underlying audio data is a local radio station broadcast that was played into the handset through an external speaker.

The first configuration we used (Figure 16) consisted of sending the output of the FH radio into a receiver. We then took the receiver intermediate frequency (IF) and connected it to the input of the IF-to-IF converter. The output of the IF-to-IF converter was then connected to the digitizer. The digitizer input was sampled at 20 MHz, 40 MHz, and 64 MHz. There are two block diagrams shown. The only difference is one IF-to-IF converter was designed and built in-house (in our office) by a government support contractor while the other is commercial off-the-shelf (COTS). The IF-to-IF converter takes a particular input center frequency (21.4 MHz) and converts it to a lower center

frequency (3.0 Mhz for the in-house or 3.225 MHz for the COTS converter). This lower center frequency allows a number of sample frequencies to be used to digitize the FH signal. The particular IF-to-IF converters used were designed to interface to a digital tape recorder that has a maximum bandwidth of 6 MHz. This limitation forces the 8 MHz input bandwidth to be bandlimited to an output bandwidth of 6 MHz.

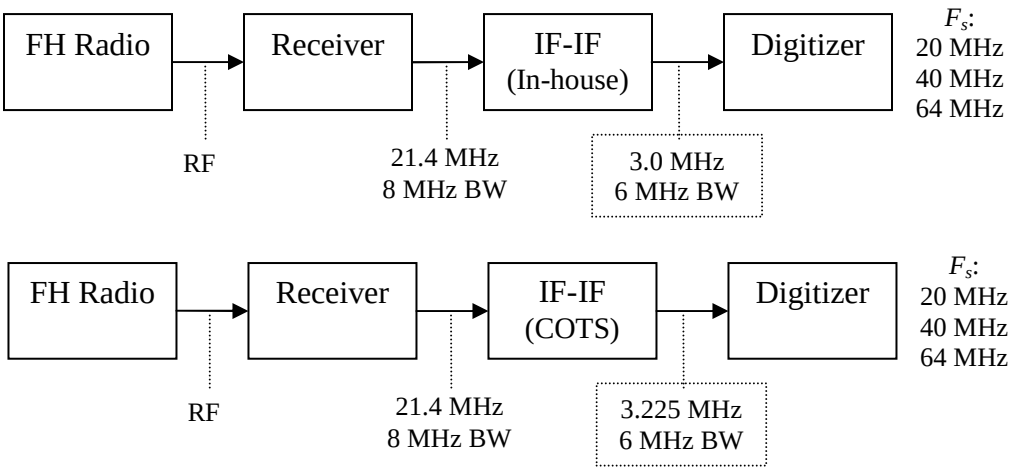

Figure 16. Block diagram of digitizing scheme with receiver and IF-to-IF converter.

All input and output points are labeled to reflect the frequency and bandwidth of the FH signal spectrum at any given point. The output of the IF-to-IF converters is boxed with a dotted line. This highlights the change in the output frequency and output bandwidth. Note that the output bandwidth of each IF-to-IF converter is approximately 6 MHz. This is less than the 6.4 MHz bandwidth of the FH signal and can cause hops to be filtered from the spectrum if they occur close enough to the bounds of the filter.

The spectra shown in Figure 17 experience a nonlinear amplitude response across the hop-band. This is a result of the signals being bandlimited to 6 MHz by output filters with a nonlinear magnitude response in the IF-to-IF converters. Each spectral plot shown in this section contains two spectrum analyzer traces. The lower trace is an actual hop of the FH signal while the upper trace shows all of the hops superimposed, as obtained using the *maxhold* feature in the software interface for the digitizer. With the possibility of hops being lost and the amplitude varying over the frequency range, this method for digitizing is not desired.

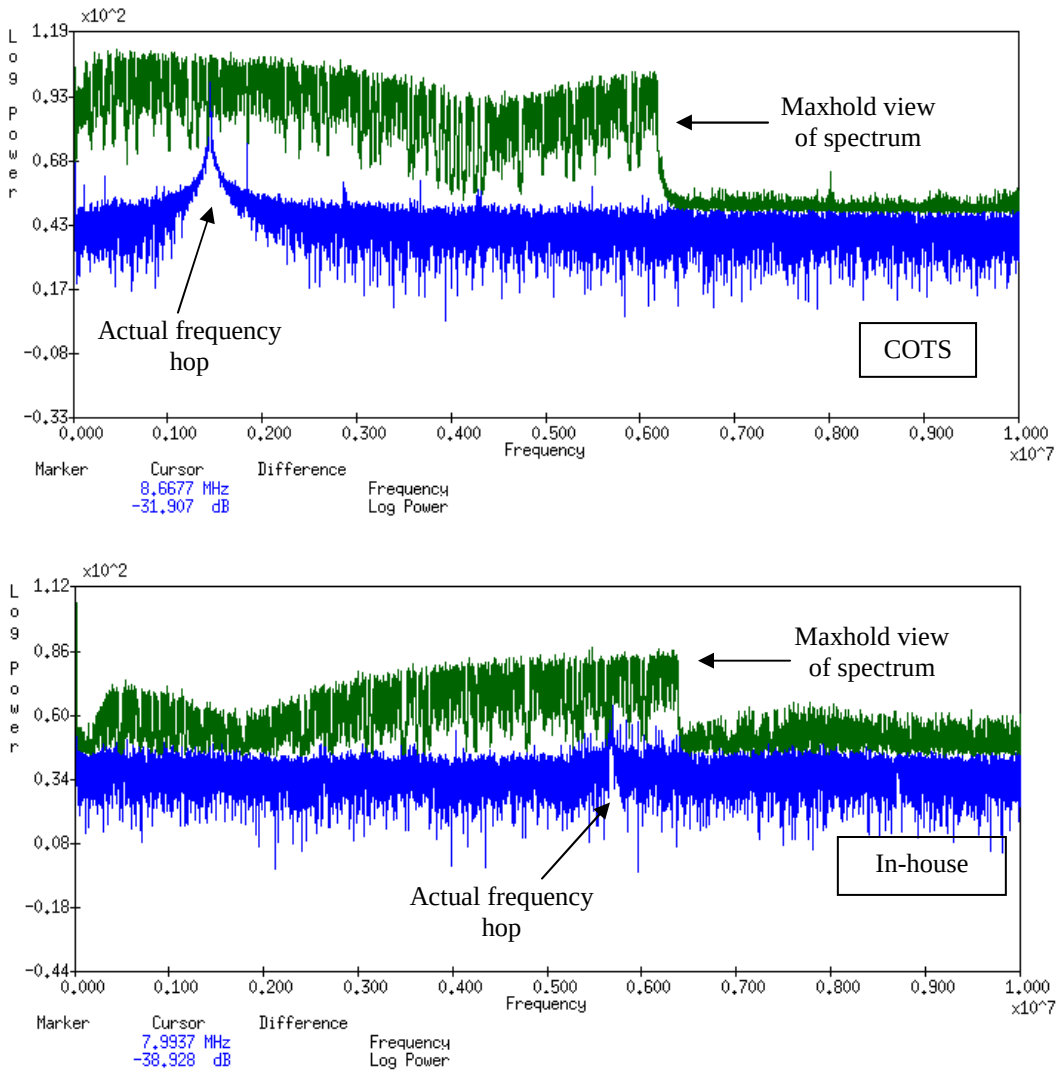

Figure 17. Spectra of FH signal through IF-to-IF converters with digitizer F_s: 20 MHz.

The next method we tried takes the IF-to-IF converters out of the configuration and relies solely on the output of the receiver (see Figure 18). The receiver output is filtered internally before it reaches the input of the digitizer. This bandwidth is wide enough to preserve all the hops that pass through the receiver.

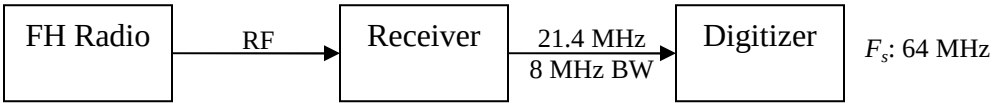

Figure 18. Block diagram of digitizing scheme with receiver only.

The resulting spectrum (Figure 19) has a linear magnitude response across the hop band, a direct result of removing the IF-to-IF converters. The entire 6.4 MHz hop band is denoted to show that all of the hops are contained in the spectrum. This result is favorable since there is little noise in the spectrum and all the hops are preserved.

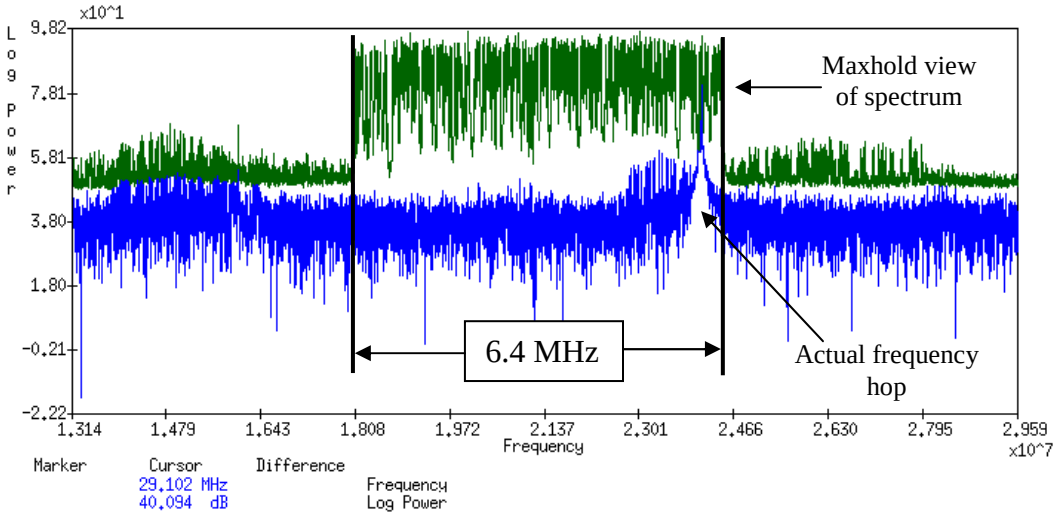

Figure 19. Spectrum of FH signal through a receiver with digitizer F_s: 64 MHz.

The final configuration we attempted involved connecting the FH radio output directly to the digitizer (see Figure 20). None of the output frequencies of the FH radio were low enough in frequency to allow the digitizer to sample at the Nyquist rate. This scheme required using the folding frequency of the digitizer to fold the hops back into the spectrum of the digitizer.

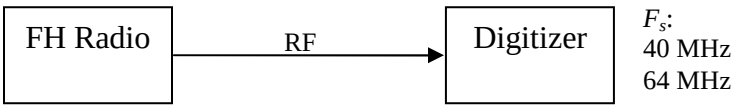

Figure 20. Block diagram of FH radio and digitizer only.

The spectrum shown in Figure 21 is the cleanest of the digitized FH signals. This is a direct result of bypassing the receiver and IF-to-IF converters, which introduce noise

into the system. Since the hops are folded back into the spectrum, the lowest frequency in Figure 21 corresponds to the highest frequency transmitted out of the radio.

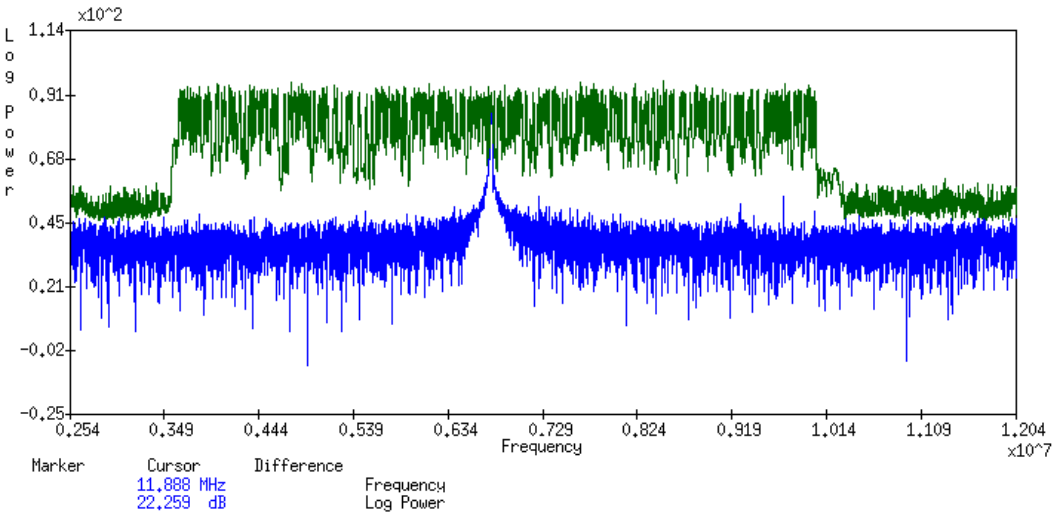

Figure 21. Spectrum of FH signal put directly into digitizer with F_s = 64 MHz.

Comparing the spectra of Figure 19 and Figure 21, we see that there are minimal differences. Further research needs to be conducted to determine the effect that using the folding frequency to digitize has on the underlying data.

D. DIGITIZING THE WIDEBAND MODE

Attempts to digitize the wideband (WB) mode (60 MHz bandwidth) of the FH radio proved unsuccessful. The widest bandwidth receiver available had a maximum bandwidth of 20 MHz, which was not sufficient for the WB signal. The fastest digitizer available had a maximum sampling frequency of 150 MHz. This would be sufficient if the WB signal could be downconverted to approximately a 30 MHz center frequency, however, no downconverter with an instantaneous bandwidth of 60 MHz was available. A digitizer with a 200 MHz sampling frequency would ensure that the WB signal could be digitized without aliasing. Digitization of the WB mode will have to wait until a digitizer with a sampling frequency of 200 MHz or greater is available.

In this Chapter we discussed the methods used to obtain digital snapshots of actual frequency-hopping signals in narrowband and wideband operating modes. A brief

discussion was given regarding the folding frequency of digitizers and how they were used to obtain the snapshots.

In the next Chapter we present the conclusions and recommendations for follow-on research.

THIS PAGE INTENTIONALLY LEFT BLANK

IV. CONCLUSIONS

A number of approaches to remove follower, tone jamming signals in the bandwidth of one hop of a frequency hopping system without causing phase distortion in the received signal have been explored in this thesis. Design parameters such as filter order, amplitude response, phase response, and group delay were used to determine which approach yielded the lowest complexity solution. We designed equivalent narrow, bandstop FIR, forward processed IIR, and forward and reverse processed IIR filters, paying close attention to the phase distortion and processing delay for each. The primary objective of this research was to show how narrowband filtering FSK signals could be accomplished without significantly degrading the quality of the signal.

The FIR design proved to be the most complex due to the significant number of taps needed for implementation. This complexity also caused a considerable processing delay equal to half the number of taps in the FIR design. The forward processed IIR filter and the forward and reverse processed IIR filter designs were identical in terms of filter order. The difference was the phase response of each filter. The forward processed IIR filter caused unacceptable phase distortion in the received signal. The forward and reverse processed IIR filter provided zero phase distortion with the same number of taps. It also provides significant BER improvement (orders of magnitude) over the forward processed IIR filter.

The FM simulations did not appear to be adversely affected by filtering with forward and reverse processing. There was noticeable audio distortion in the demodulated FM signal when forward processing was used.

Further research needs to be conducted to determine the best way to filter follower jamming signals that jam one of the FSK signal tones. Ideally, a filter designed with a null depth equal to the amplitude of the received jamming signal would effectively eliminate the jammer. It would also be interesting to design the null depth slightly above and slightly below the received jamming amplitude to see what effect overestimating and underestimating the received jamming amplitude has on the system performance. Since

forward and reverse processing squares the magnitude response of the IIR filter, the null depth of the IIR filter would have to be equal to the square root of the received jamming signal amplitude.

LIST OF REFERENCES

[1] Website, “The Frequency Hopping Concept,” [www.hedylamarr.at/freqHopping1e.html], September 2001.

[2] Mary Ann Hoffman, “Hedy Lamarr,” IEEE History Center website, [www.ieee.org/organizations/history_center/lamarr.html], August 2002.

[3] Martin Ruengert, Sean Gannon, “A2C2S MCE/Communications Tutorial,” Rev A., Federation of American Scientists website, [www.fas.org/man/dod-101/sys/ac/equip/docs/A2C2S_Tutorial_RevA1a/sld017.htm], January 1999.

[4] R. Clark Robertson and Joseph F. Sheltry, “Multiple Tone Interference of Frequency-hopped Noncoherent MFSK Signals Transmitted Over Ricean Fading Channels,” *IEEE Transactions on Communications*, Vol. 44, No. 7, pp. 867-875, July 1996.

[5] George Katsoulis and R. Clark Robertson, “Performance Bounds for Multiple Tone Interference of Frequency-hopped Noncoherent MFSK Systems,” *Proceedings IEEE Military Communications Conference*, pp. 307-312, *IEEE*, New York, 1997.

[6] J.J. Pérez, M.A. Rodriguez, and S. Felici, “Interference Excision Algorithm for Frequency Hopping Spread Spectrum Based on Undecimated Wavelet Packet Transform,” *Electronics Letters*, Vol. 38, No. 16, pp. 9114-915, August 2002.

[7] Laurence B. Milstein, “Interference Rejection Techniques in Spread Spectrum Communications,” *Proceedings of the IEEE*, Vol. 76, No. 6, pp. 657-671, June 1998.

[8] M. J. Bouvier, Jr., “The Rejection of Large CW Interferers in Spread Spectrum Systems,” *IEEE Trans. Commun.*, Vol. COM-28, pp. 254-256, February 1978.

[9] A. E. S. Mostafa, M. Abdel-Kader, and A. El-Osmany, “Improvements of Anti-jam Performance of Spread-spectrum Systems,” *IEEE Trans. Commun.*, Vol. COM-31, pp. 803-808, January 1983.

[10] Robert L. Kay, “Digital Filters – General Form,” Technical Report, Elite Engineering Corporation, Camarillo, CA, June 1996.

[11] Paul Horowitz and Winfield Hill, *The Art of Electronics*, 2nd Ed., New York: Cambridge University Press, 1989.

[12] R.I. Damper, *Introduction to Discrete-Time Signals and Systems*, London, Chapman & Hall, 1995.

INITIAL DISTRIBUTION LIST

1. Defense Technical Information Center
   Ft. Belvoir, Virginia

2. Dudley Knox Library
   Naval Postgraduate School
   Monterey, California

3. Chairman, Code EC
   Department of Electrical and Computer Engineering
   Naval Postgraduate School
   Monterey, California

4. Professor R.Clark Robertson, Code EC/Rc
   Department of Electrical and Computer Engineering
   Naval Postgraduate School
   Monterey, California

5. Professor Tri T. Ha, Code EC/Ha
   Department of Electrical and Computer Engineering
   Naval Postgraduate School
   Monterey, California

6. Kyle Kowalske
   7001 Gentle Shade, Apt. 304
   Columbia, MD 21046

7. Kevin Waters
   510 Glenview Ave.
   Glen Burnie, MD 21061